Loto & Babalola, *Cogent Engineering* (2017), 4: 1422229
https://doi.org/10.1080/23311916.2017.1422229

cogent engineering

MATERIALS ENGINEERING | RESEARCH ARTICLE

Corrosion polarization behavior and microstructural analysis of AA1070 aluminium silicon carbide matrix composites in acid chloride concentrations

Roland Tolulope Loto[1]* and Philip Babalola[1]

Abstract: The effect of SiC content and NaCl concentration on the corrosion resistance of AA1070 aluminium in 2 M H_2SO_4 was evaluated with potentiodynamic polarization technique, open circuit potential measurement (OCP) and optical microscopy. Results showed SiC increased the corrosion susceptibility of the alloy at lower NaCl concentrations compared to results obtained at 0% NaCl which showed significant decrease in corrosion rates, with maximum inhibition efficiency of 90.84% at 20% SiC content. The corrosion rates decreased at higher NaCl concentration, with maximum inhibition efficiency of 94.12 and 77.27% at 20% SiC. Alloy samples in 2 M H_2SO_4/0% NaCl at 0 and 20% SiC visibly decreased in OCP value over wide variation compared to samples with varying NaCl concentration due to loss of passivity. OCP values for alloys at varying NaCl concentration decreased over a very short variation due to repassivation. Statistical data showed silicon carbide to be the only relevant variable responsible for the corrosion rate values with F-values of 8.85 corresponding to a percentage significance of 54.8%. Optical images showed the presence of corrosion pits of smaller dimension, yet deeper on the morphology of the alloy without silicon carbide compared the alloy containing it, whose corrosion pits, seems wider but very shallow.

Received: 16 November 2017
Accepted: 20 December 2017
First Published: 29 December 2017

*Corresponding author: Roland Tolulope Loto, Department of Mechanical Engineering, Covenant University, Ota, Ogun State, Nigeria
E-mail: tolu.loto@gmail.com

Reviewing editor:
Julio Sánchez, Universidad de Santiago de Chile, Chile

Additional information is available at the end of the article

ABOUT THE AUTHORS

Roland Tolulope Loto is a professor at the Department of Mechanical Engineering, Covenant University, Ota, Ogun State, Nigeria. He is the principal investigator of the corrosion and materials research cluster. Roland has over 80 research publications including reviews in top international journals and has consistently served as reviewer in respectable journals due to his in-depth knowledge and technical expertise. Roland is a registered member of the Council for the Regulation of Engineering in Nigeria, South African Institute of Mining and Metallurgy and the Corrosion Institute of Southern Africa.

Philip Babalola (PhD) is a lecturer at the Department of Mechanical Engineering, Covenant University, Ota, Ogun State, Nigeria. He specializes in research on composites, renewable energy applications, pipe network analysis with significant publications. He is a registered member the Council for Regulation of Engineering in Nigeria and corporate member of the Nigerian Society of Engineers.

PUBLIC INTEREST STATEMENT

The economic impact and problems resulting from corrosion has drawn strong attention from scientists and engineers worldwide. Corrosion of aluminium alloys in industrial environments is a major concern in chemical processing plants, oil and gas industry, manufacturing and automobile industry, marine operations, boiler and power generation plants due to the considerable cost involved in the replacement of metallic parts in their various applications. The consequence often leads to plant shutdowns, breakdown of industrial equipment, reduced efficiency, industrial downtime, high maintenance cost due to replacement of damaged part, wastage of valuable resources and expensive overdesign. Corrosion prevention through modification of the metallurgical structure of aluminium with the addition of silicon carbide is of great practical importance and can be extensively employed in curtailing wastage of engineering materials and minimizing costs of corrosion control.

Subjects: Material Science; Materials Science; Metals & Alloys; Composites; Corrosion-Materials Science; Surface Engineering-Materials Science

Keywords: corrosion; aluminium; SiC, NaCl; composite

1. Introduction

1070 aluminium alloy is widely used for general industrial components, in building and construction, communication cables, heat exchangers, corrosion resistant vessels and tanks, chemical industry and for joining pieces of aluminium. The electrochemical properties of this aluminium grade can be greatly enhanced with the addition of reinforcements in the form of ceramic such as SiC precipitates (Birol, 2007; Zou, Miyahara, Yamamoto, & Ogi, 2003). Aluminium alloys are known to be widely used due to their low density to weight ratio, high strength and corrosion resistance property in chemical processing industries, aerospace, automotive, thermal control applications etc. Their extensive property exposes them to degradation in the presence of corrosive anions (Alaneme, Olubambi, Afolabi, & Bodurin, 2014; Asif, Chandra, & Misra, 2011; Prasad, Shoba, & Ramanaiah, 2014). Corrosion studies of aluminium and aluminium alloys have received considerable attention by researchers in recent years. Reports have shown that intermetallic precipitates influence the corrosion behavior of aluminum alloys. These precipitates may interact with the aluminium matrix leading to reduced or increased corrosion resistance of the alloy (Abbas, 2010; Ambat, Davenport, Scamans, & Afseth, 2006; Bodunrin, Alaneme, & Chown, 2015; Christian, 2004; Guillaumin & Mankowski, 2000; Paciej & Agarwala, 1986). Most often the presence of reinforcements hinders the continuity of the aluminum alloy and the surface oxide film due to the occurrence of galvanic couples at the boundary/interface between the aluminium substrate and the precipitates of the reinforcing material. This increases the number of sites where redox electrochemical reactions are more likely occur (Aziz, Qi, & Min, 2009; Deuis, Green, Subramanian & Yellup, 1997; Trowsdale et al., 1996). The effect of corrosion in matrix composite is also subject to the prevailing environmental conditions and processing methods which alters the microstructure. The processing methods and composite size affects void size and content, dislocation density and precipitation of active phases in aluminium matrices due to reinforcement/matrix reactions forming new inter metallic phase (Gopinath, Balasubramaniam, & Murthy, 2001; Trzaskoma, 1990). Previous research has been done on aluminium matrix composites based on the 2xxx, 6xxx and 7xxx series, but research on aluminium matrix composites based on 1xxx series is scarce (Alaneme & Bodunrin, 2011; Dobrzański, Włodarczyk, & Adamiak, 2005; Ehsani & Reihani, 2004; Gharavi, Matori, Yunus, Othman, & Fadaeifard, 2015; Reena Kumari, Nayak, & Nityananda Shetty, 2016). In contribution to research on aluminium matrix composites, this research aims to study the corrosion resistance of 1070 aluminium matrix composite sand casted from an oil fired tilting furnace in dilute sulphuric acid at specific concentrations of NaCl.

2. Experimental methods

2.1 Materials and preparation

AA1070 aluminium ingot (1070AL) obtained from Aluminium Rolling Mills, Ota, Ogun State, Nigeria has a nominal (wt. %) composition presented in Table 1. Silicon carbide (SiC) of 320 grit size obtained from Logitech, UK, with nominal (wt. %) composition shown in Table 2 was used to reinforce 1070AL at weight percentages of 10, 15 and 20%. 1070AL was melted in a tilting furnace of 20 kg capacity for 45 min at a temperature of 650°C. SiC was added to the liquid 1070AL, stirred mechanically and cast into sand moulds. The process was repeated for each specified percentage of SiC. The cast samples (1070AL/SiC) were allowed to cool for 24 h, then grinded with silicon carbide papers (80, 320,

Table 1. Nominal (wt. %) composition of 1070AL

Element symbol	Fe	Si	Mn	Cu	Zn	Ti	Mg	Pb	Sn	Al
% Composition	0.232	0.078	0.000	0.0006	0.0016	0.006	0.0027	0.0012	0.007	99.66

Table 2. Nominal (wt. %) composition of SiC

Element symbol	C	Al	Fe	Si	SiO_2	Magnetic Fe	SiC
% Composition	0.50	0.30	0.20	0.80	0.0016	0.04	97.6

Table 3. Brinell hardness test results

Material	Brinell hardness
100% Al	133.37
10% SiC + 90% Al	138.08
15% SiC + 85% Al	150.15
20% SiC + 80% Al	216.3

600, 800 and 1,000 grit) after machining, cleansed with deionized water and propanone, and kept in a desiccator for electrochemical test and corrosion potential measurement according to ASTM G1-03 (2011). Recrystallized NaCl obtained from Titan Biotech, India was prepared in volumetric concentrations of 0, 0.25, 0.5, 0.75 and 1% in 200 mL of 2 M H_2SO_4 solution, prepared from analar grade of H_2SO_4 acid (98%) with deionized water. 1070AL/SiC was indented with a 10 mm diameter hardened steel/carbide ball subjected to a load of 3000 kg for 30 s. The diameter of the indentation left in the test material was measured with a low powered microscope. The Brinell hardness number was calculated by dividing the load applied by the surface area of the indentation to give the hardness test results in Table 3.

2.2 Potentiodynamic polarization technique

Polarization measurements were carried out at ambient temperature of 37°C using a three electrode system and aerated glass cell containing 200 mL of the corrosive test solution with Digi-Ivy 2311 electrochemical workstation. 1070AL/SiC electrodes mounted in acrylic resin with an exposed surface area of 1 cm^2 were prepared according to ASTM G59-97 (2014). Polarization plots were obtained at a scan rate of 0.0015 V/s between potentials of −0.75 and +1.5 V according to ASTM G102-89 (2015). A platinum rod was used as the counter electrode and a Fisher Scientific standard silver chloride electrode (Ag/AgCl) as the reference electrode. Corrosion current density (j_{cr}) and corrosion potential (E_{cr}) values were obtained using the Tafel extrapolation method. The corrosion rate, C_R (mm/y) and the inhibition efficiency, η (%) were calculated from the mathematical relationship;

$$C_R = \frac{0.00327 \times J_{cr} \times E_{qv}}{D} \quad (1)$$

where j_{cr} is the current density (A/cm^2), D is the density (g/cm^3), E_{qv} is the sample equivalent weight (g). 0.00327 is a constant for corrosion rate calculation (Basics of Corrosion Measurements, xxxx).

2.3 Open circuit potential measurement

OCP measurements were obtained at a step potential of 0.05 V/s with two-electrode electrochemical cell consisting of silver chloride reference electrode and resin mounted 1070AL/SiC (exposed surface of 1 cm^2) as the working electrode, connected to Digi-Ivy 2311 potentiostat. The electrodes were fully immersed in 200 ml of the test media at specific concentrations of 2 M H_2SO_4/NaCl concentrations for 2,400 s.

2.4 Optical microscopy characterization

Optical images of the corroded and inhibited 1070AL/SiC surface morphologies were obtained and analysed after the electrochemical test with Omax trinocular with the aid of ToupCam analytical software.

3. Results and discussion

3.1 Potentiodynamic polarization test

The effect of silicon carbide content and NaCl concentration on the electrochemical characteristics of 1070AL/SiC in 2 M H_2SO_4 from potentiodynamic polarization technique is shown in Figure 1(a)–(e). Table 4 shows the results of the polarization scans. At 0% NaCl concentration on Table 4, a significant decrease in corrosion rate is observed with increase in SiC concentration from 0.87 mm/y (0% SiC) to 0.08 mm/y (20% SiC). The presence of SiC improved the corrosion resistance of 1070AL/SiC in the absence of Cl^- ions. SiC inhibits the electrochemical action of SO_4^{2-} ions on 1070AL/SiC surface in the acid solution through the formation of SiO_2 in 1070AL/SiC matrix. This strengthens the passivation resistance of the alloy, resulting in a maximum inhibition efficiency of 90.84% at 20% SiC content. There is the possibility that the aluminium oxide film grows homogeneously on the metal surface through simultaneous migration of O anions and oxidized aluminium atoms resulting from the electric field generated by the applied potential across the film. The corrosion potential shifts to cathodic values due to the dominant cathodic inhibiting action of SiC in 1070AL/SiC whereby the hydrogen evolution and oxygen reduction reactions are effectively suppressed. The presence of SiC precipitates increased the surface impedance of the 1070AL/SiC. Addition of SiC to 1070AL/SiC had no significant effect on the cathodic Tafel slopes. The anodic Tafel slopes are slightly greater than the cathodic Tafel slopes due to the anodic exchange current density values being lesser than the cathodic values.

Addition of Cl^- ion concentration to the acid solution caused a remarkable change in the electrochemical behaviour of 1070AL/SiC. At 0.25 and 0.5% NaCl concentrations, the corrosion rate of 1070AL/SiC increases with increase in SiC concentration due to breakdown of oxide film on the surface, resulting in nil inhibition efficiency. The SiC composite tends to be cathodic to the aluminium matrix in the presence of low Cl^- ion concentration, possibly due to the difference in coefficients of thermal expansion between the aluminium matrix and SiC composite which generates higher dislocation density responsible for the increase in corrosion rate (Bodunrin et al., 2015; Singh & Chauhan, 2016). These sites on the alloy surface are most likely to be the area where the oxide film discontinues, directly exposing the aluminium substrate metal to the corrosive anions. The corrosion rates of 1070AL/SiC at 0.5% NaCl are relatively higher than the values at 0.25% NaCl however active-passive polarization can be observed on their polarization plots (Figure 1(b) and 1(c)) due to changes in the redox electrochemical behaviour of the alloy. This coincides with visible changes in the cathodic and anodic Tafel slopes, and corrosion potential values with respect to variation in SiC content due to localized breakdown of the passivating oxide film by Cl^- ions as earlier explained. The shifts in corrosion potential indicate the loss of passivity of 1070AL/SiC due to thinning of primary oxide layer as a result of the chemical dissolution action of SO_4^{2-} and Cl^- ions. The oxide layer consists of amorphous γ alumina which initially thickens on exposure to neutral aqueous solution with the formation of a layer of crystalline hydrated alumina. The small size of Cl^- ions enables penetration through the passive oxide film under the effect of an electric field. They induce localized dissolution of the passivating oxide film at some discontinuity such as a grain boundary, dislocation or inclusion in the metal. Further increase in NaCl concentration beyond 0.5% NaCl results in a decrease in corrosion rate values at 0.75 and 1% NaCl concentration with increase in SiC content, however the inhibition efficiency values at 0.75% NaCl is quite higher than the values in 1% NaCl. The negative shift in the corrosion potential with increase in SiC concentration indicates that the cathodic process dominates relative to the anodic process. It shows the dependence of 1070AL/SiC corrosion resistance to changes in Cl^- ion concentration.

Comparison of the corrosion rate results of 1070AL/SiC at 0% SiC content for 0–1% NaCl concentration shows that increase in Cl^- concentration (0.25–0.5% NaCl) decreases the corrosion rate of 1070AL/SiC after which there is a sudden increase in corrosion rate value at 0.75–1% NaCl. The presence of SiC in 1070AL in the presence of Cl^- ions tends to have opposite effect on 1070AL/SiC. SiC with 1070AL matrix causes an increase in corrosion rate values at 0.25% and 0.5% NaCl despite a relative decrease in corrosion rate for 1070AL sample at 0% SiC content. But at higher NaCl

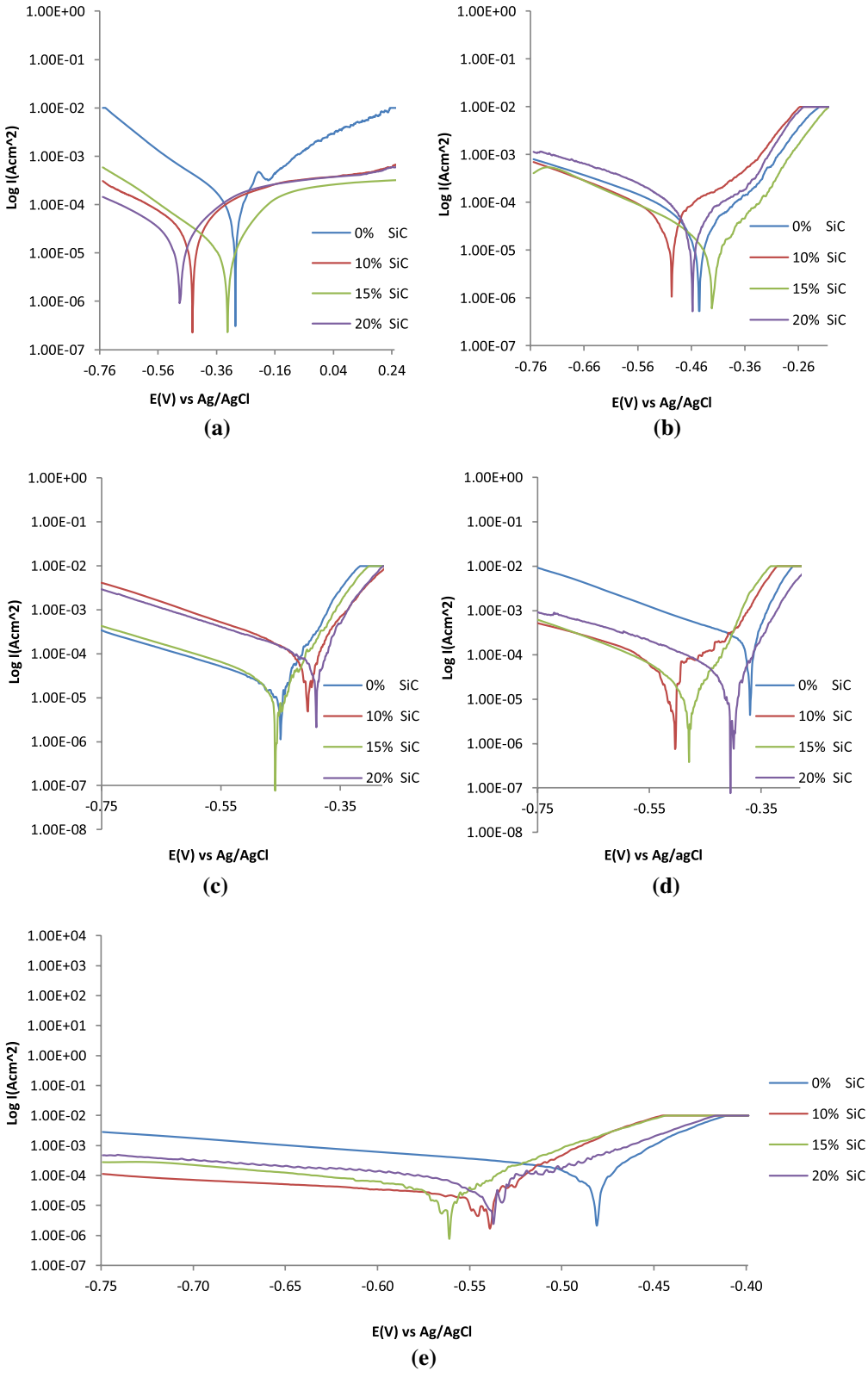

Figure 1. Potentiodynamic polarization plots for 1070AL/SiC in 0.2 M HCl at (a) 0% NaCl, (b) 0.25% NaCl, (c) 0.5% NaCl, (d) 0.75% NaCl and (e) 1% NaCl concentrations.

Table 4. Potentiodynamic polarization results for 1070AL/SiC in 0.2 M H_2SO_4 at 0, 0.25, 0.5, 0.75 and 1% NaCl concentrations

Sample	SiC conc. (%)	Corrosion rate (mm/y)	Inhibition efficiency (%)	Corrosion current (A)	Corrosion current density (A/cm²)	Corrosion potential (V)	Polarization resistance, *Rp* (Ω)	Cathodic tafel slope, B_c (V/dec)	Anodic tafel slope, B_a (V/dec)
0% NaCl									
A	0	0.87	0	7.99E-05	7.99E-05	−0.296	321.5	−5.928	6.42
B	10	0.2	76.45	1.88E-05	1.88E-05	−0.443	1365	−5.413	6.415
C	15	0.1	89.08	8.73E-06	8.73E-06	−0.323	2944	−5.839	8.632
D	20	0.08	90.84	7.32E-06	7.32E-06	−0.485	3548	−5.521	8.802
0.25% NaCl									
A	0	0.32	0	2.94E-05	2.94E-05	−0.44	875.3	−6.546	8.497
B	10	0.41	0	3.79E-05	3.79E-05	−0.492	1043.7	−5.641	4.963
C	15	0.48	0	4.42E-05	4.42E-05	−0.415	1358	−6.85	10.25
D	20	0.52	0	4.79E-05	4.79E-05	−0.453	1836.6	−7.007	6.669
0.5% NaCl									
A	0	0.49	0	4.50E-05	4.50E-05	−0.45	570.8	−4.959	27.24
B	10	0.83	0	7.67E-05	7.67E-05	−0.404	365.8	−6.202	17.96
C	15	1.06	0	9.78E-05	9.78E-05	−0.459	224.8	−5.272	20.59
D	20	1.49	0	1.37E-04	1.37E-04	−0.39	187.2	−5.227	16.64
0.75% NaCl									
A	0	4.11	0	3.78E-04	3.78E-04	−0.37	68.02	−3.866	9.218
B	10	0.7	82.89	6.46E-05	6.46E-05	−0.504	397.9	−7.335	8.851
C	15	0.25	93.89	2.31E-05	2.31E-05	−0.479	1115	−6.876	27.41
D	20	0.24	94.12	2.22E-05	2.22E-05	−0.405	1157	−5.686	22.56
1% NaCl									
A	0	3.17	0	2.92E-04	2.92E-04	−0.482	88.15	−4.673	4.827
B	10	0.88	72.25	8.08E-05	8.08E-05	−0.54	318	−4.378	21.03
C	15	0.84	73.66	7.67E-05	7.67E-05	−0.562	385.2	−6.164	19.71
D	20	0.72	77.27	6.62E-05	6.62E-05	−0.542	437.2	−3.49	20.07

cogent engineering

concentration (0.75 and 1% NaCl) the corrosion rate of 1070AL/SiC decreases despite significant increase in corrosion rate for 1070AL at 0% SiC. These observations is due to the simultaneous reaction of aluminum in the acid solution at varying NaCl concentrations resulting in the formation of hydroxide film on its surface through incorporation and diffusion of ions into the film, while at the same time anodic dissolution at the film/solution interface occurs. With respect to Cl^-/SO_4^{2-} ion ratio and SiC content, the dominant reaction tends to determine the overall corrosion resistance of 1070AL/SiC. There is possibility that galvanic corrosion between 1070AL matrix and SiC reinforcement occurs which may form micro-galvanic cells and induce localized corrosion

3.2 OCP measurement

The OCP values for 1070AL/SiC samples in the acid chloride solution are shown in Figure 2. 1070AL/SiC samples in 0% NaCl at 0 and 20% SiC content visibly decreased in OCP value over a wide variation compared to other samples with varying NaCl concentration at the first 800s of exposure. The decrease in OCP value indicates the loss of passivity of the specimen due to thinning of primary oxide layer by the chemical dissolution action of SO_4^{2-}. The OCP variation for 1070AL/SiC at 20% SiC is much smaller and its value tends to increase after 500s of exposure till 2400s due to repassivation of the protective oxide layer and the presence of SiO_2 on the alloy surface. The passive film of 1070AL/SiC at 0% SiC/0% NaCl continued to thin out exposing the substrate 1070AL metal as shown in its OCP value whose rate of decrease in value slowed down but continued till 2400s. The difference in electrochemical behaviour for the alloy specimens at 0% NaCl is due to the presence is clearly due to the presence of SiC in the alloy sample thus 1070AL/SiC at 20% SiC content has a lower thermodynamic tendency to corrode.

It is observed that the OCP values for 1070AL/SiC at varying NaCl concentration decreased over a very short variation from 0s to between 116s and 196s before increasing to OCP values between −0.515 V and −0.520 V at 480s-620s due to the relatively instantaneous repassivation of the protective film. The OCP values afterwards remained relative constant over short potential ranges but thermodynamically unstable till the end of the exposure hours at 2400s due to continuous fluctuations. The fluctuation of OCP values in the manner observed is typical of materials systems undergoing repeated passive film formation and breakdown due to exposure to a corrosive environment, however 1070AL/SiC at 20% SiC content in 0.25% NaCl concentration solution showed the highest corrosion resistance due to its relatively higher OCP values resulting from a wider shift in the positive direction, followed by 1070AL/SiC at 20% SiC content in 0.5% NaCl, 0.75% NaCl and 1% NaCl. This observation shows that without applied potential Cl^- ion concentration influences the corrosion resistance and thermodynamic stability of 1070AL/SiC alloy on chloride containing environments.

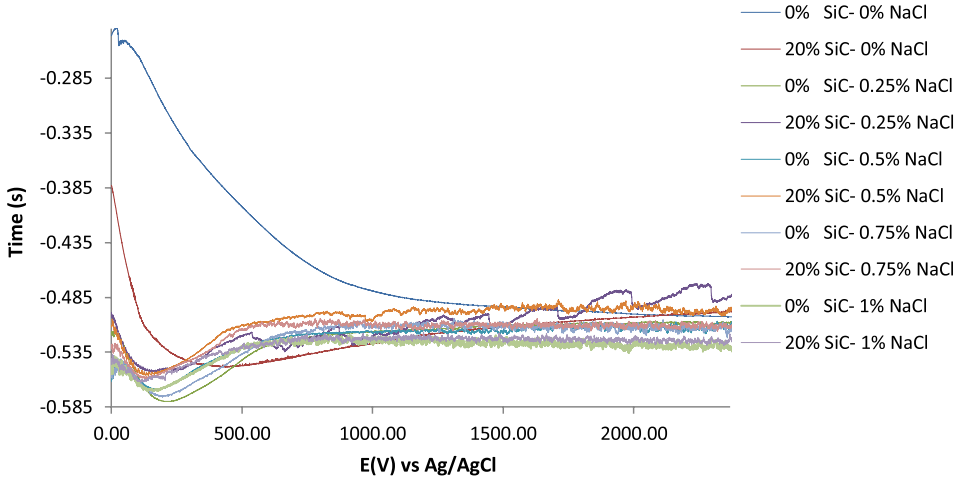

Figure 2. Variation of corrosion potential with time for 1179AL/SiC specimens immersed in 0.2 M H_2SO_4 at 0, 0.25, 0.5, 0.75, 1% NaCl concentrations.

3.3 Optical microscopy analysis

The optical microscopic images of 1070AL/SiC samples before and after the electrochemical tests are shown from Figures 3(a)–7(c). Figure 3(a)–(d) shows the optical images of 1070AL/SiC samples at 0, 10, 15 and 20% SiC content before the corrosion test. The morphology of 1070AL/SiC at 0% SiC content shows the presence of visible impurities in the microstructure of the aluminium metal substrate before heat treatment. The impurities gradually disappeared with increase in SiC content (Figure 3(b) and (c)) after heat treatment. Figure 4(a)–(c) shows the morphology of 1070AL/SiC at 0% SiC content from 2 M H_2SO_4/0, 0.5 and 1% NaCl solution. The morphology of 1070AL/SiC sample from 2 M H_2SO_4/0% NaCl (Figure 4(a)) corroded slightly in comparison to its morphology before corrosion (Figure 3(a)). The visible impurities seem to have drastically reduced in number with the fewer remaining ones enlarged in size. 1070AL/SiC from 2 M H_2SO_4/0.5% NaCl (Figure 4(b)) solution showed the presence of macro-pits due to the action of Cl^- ions resulting in localized corrosion of 1070AL/SiC surface. In 2 M H_2SO_4/1% NaCl solution the alloy morphology the showed the presence of much smaller macro-pits probably due to competitive action of Cl^- ions resulting from excessive Cl^- ions.

1070AL/SiC morphologies at 10% SiC content from 2 M H_2SO_4/0, 0.5 and 1% NaCl solution (Figure 5(a) and (b)) contrast its morphology before corrosion (Figure 3(b)). Figure 5(a) showed a marginally corroded image while Figure 5(b) showed a worn out morphology with a shallow macro-pit compared to Figure 5(c) whose macro-pit appears smaller but deeper and the surrounding alloy surface seems less corroded. Similar observations were confirmed for 1070AL/SiC samples at 15 and 20% SiC content from 2 M H_2SO_4/0, 0.5 and 1% NaCl solution (Figures 6 and 7). The most significant contrast in the optical images results from comparison of 1070AL/SiC at 0% SiC content and 1070AL/SiC at 10, 15 and 20% SiC content from 2 M H_2SO_4/0.5% NaCl solution probably due to the presence of SiC at varying concentration. The presence of SiO_2 on the alloy surface, resulting from the oxidation of SiC is a major contributing factor to the observed surface morphologies. 1070AL/SiC at 0% SiC content had relatively smaller but deeper micro-pits compared to the earlier mentioned samples where the corrosion pits a quite larger but shallow.

3.4 Statistical analysis

Statistical analysis through analysis of variance (ANOVA) at a confidence level of 95% (significance level of $\alpha = 0.05$) was used to calculate the statistical relevance of SiC content and NaCl concentration on the obtained corrosion rate values of 1070AL 2 M H_2SO_4 solutions according to Equations (2)–(4).

The Sum of squares among columns (NaCl concentration)

$$SS_c = \frac{\sum T_c^2}{nr} - \frac{T^2}{N} \tag{2}$$

Sum of Squares among rows (SiC content)

$$SS_r = \frac{\sum T_r^2}{nc} - \frac{T^2}{N} \tag{3}$$

Total Sum of Squares

$$SS_{Total} = \sum x^2 - \frac{T^2}{N} \tag{4}$$

The statistical data in Table 5 showed that SiC is the only relevant statistical variable responsible for 1070AL corrosion rate values with *F*-values of 8.85. This value is significantly greater than the theoretical significance factor (significance *F*) value of 3.49, corresponding to a percentage significance of 54.8%.The statistical value of NaCl concentration at 2.47 is quite below the theoretical significance factor of 3.26, which equates to a percentage significance of 20.4%. The results show that SiC

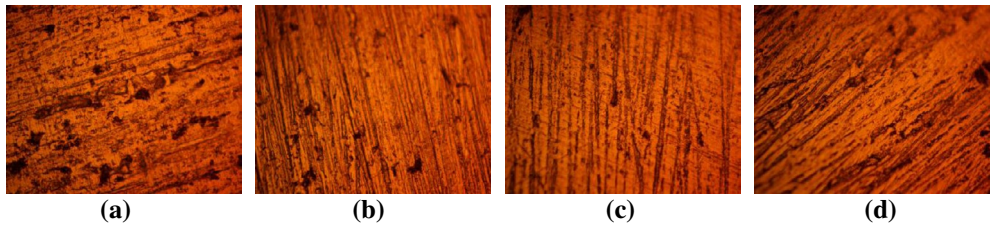

Figure 3. Optical images of 1070AL/SiC samples (mag. × 40) at 0, 10, 15 and 20% SiC content before the corrosion test.

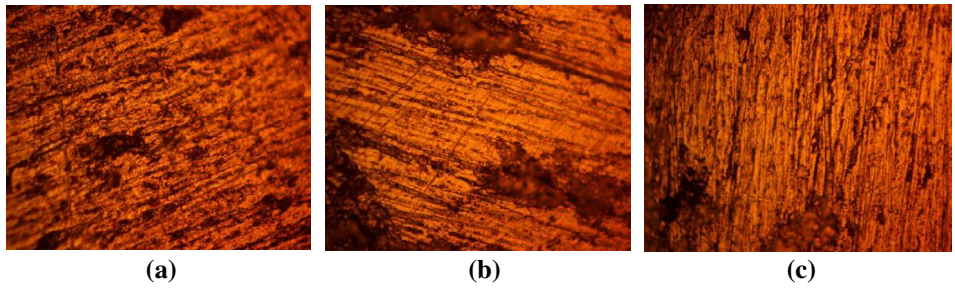

Figure 4. Morphology of 1070AL with 0% SiC content from 2 M H_2SO_4 at (a) 0% NaCl, (b) 0.5% NaCl and (c) 1% NaCl solution.

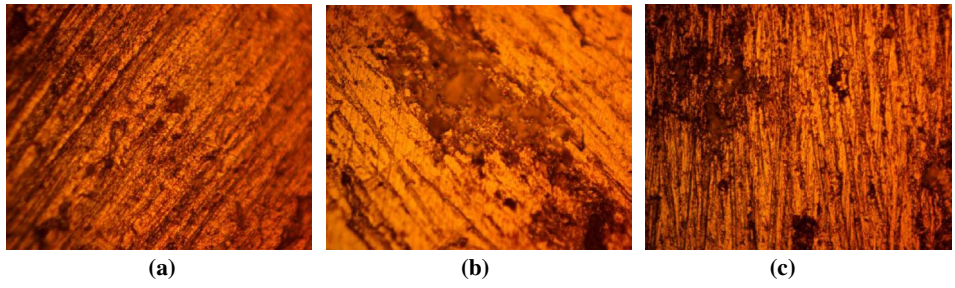

Figure 5. Morphology of 1070AL with 10% SiC content from 2 M H_2SO_4 at (a) 0% NaCl, (b) 0.5% NaCl and (c) 1% NaCl solution.

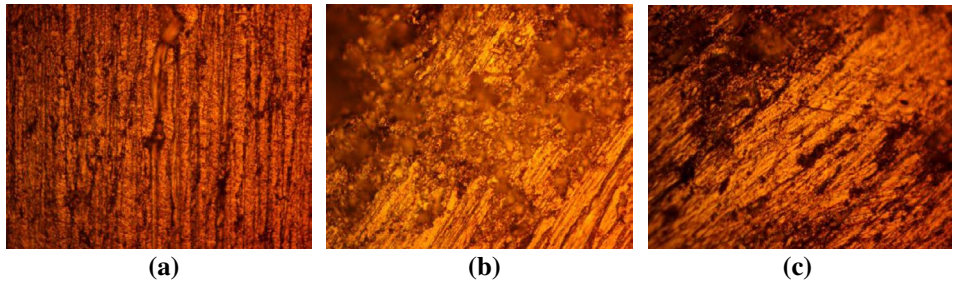

Figure 6. Morphology of 1070AL with 15% SiC content from 2 M H_2SO_4 at (a) 0% NaCl, (b) 0.5% NaCl and (c) 1% NaCl solution.

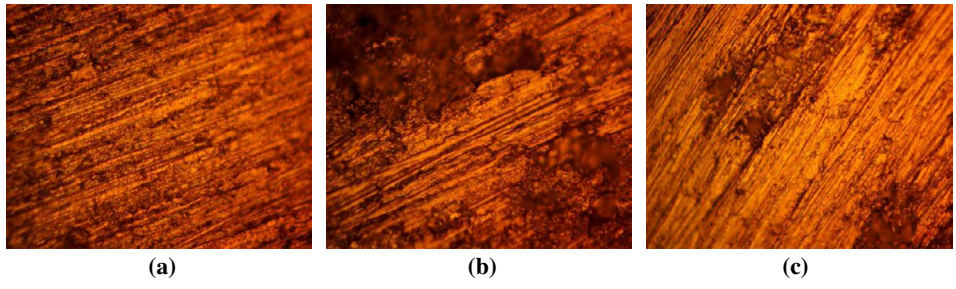

Figure 7. Morphology of 1070AL with 20% SiC content from 2 M H_2SO_4 at (a) 0% NaCl, (b) 0.5% NaCl and (c) 1% NaCl solution.

Table 5. Analysis of variance for 1070AL/SiC in 2 M H_2SO_4/(0–1% NaCl) at 95% confidence level

Source of variation	Sum of squares	Degree of freedom	Mean square	Mean square ratio (*F*)	Significance *F*	*F* (%)
NaCl concentration	4.00	4	1.00	2.47	3.26	20.4
SiC content	10.77	3	3.59	8.85	3.49	54.8
Residual	4.86	12	0.41			
Total	19.64	19				

content has strong influence on the electrochemical characteristics and the resulting microstructural properties of 1070AL in contrast to NaCl concentration whose relevance is below the significant threshold, hence SiC content is the major determinant in the corrosion resistance of 1070AL in 2 M H_2SO_4/(0, 0.25, 0.5, 0.75 and 1% NaCl) solution

4. Conclusion

SiC significantly improved the corrosion resistance of AA1070 aluminium alloy in dilute H_2SO_4 solution without the presence of NaCl and at higher NaCl concentration studied due to the formation of SiO_2 within the aluminium matrix which strengthened the oxide protective film on its surface. The cathodic shift in corrosion potential is due to the dominant cathodic inhibiting action of SiC as its precipitates increased the surface impedance of the aluminium alloy. Alloy samples in the presence chloride visibly decreased in OCP value over very short variation compared to samples without chloride due to repassivation. The OCP values remained relative constant over short potential ranges but thermodynamically unstable till the end of the exposure hours to continuous fluctuations. Statistical results showed that SiC is the only relevant statistical variable responsible for corrosion rate values of the aluminium alloy whose value is above the theoretical significance. Optical images show the presence of SiC improves the pitting corrosion resistance of the aluminium alloy.

Funding
The authors acknowledge Covenant University Ota, Ogun State, Nigeria for the sponsorship and provision of research facilities for this project.

Author details
Roland Tolulope Loto[1]
E-mail: tolu.loto@gmail.com
Philip Babalola[1]
E-mail: phillip.babalola@covenantuniversity.edu.ng
[1] Department of Mechanical Engineering, Covenant University, Ota, Ogun State, Nigeria.

Citation information
Cite this article as: Corrosion polarization behavior and microstructural analysis of AA1070 aluminium silicon carbide matrix composites in acid chloride concentrations, Roland Tolulope Loto & Philip Babalola, *Cogent Engineering* (2017), 4: 1422229.

References

Abbas, M. K. (2010). Effects of friction stir welding on the microstructure and corrosion behavior of aluminum alloy AA6061-T651. In *Proceedings of the 2nd regional conference for engineering sciences* (pp. 1–2), Baghdad.

Alaneme, K. K., & Bodunrin, M. (2011). Corrosion behavior of alumina reinforced aluminium (6063) metal matrix composites. *Journal of Minerals and Materials Characterization and Engineering, 10*(12), 1153–1165.

Alaneme, K. K., Olubambi, P. A., Afolabi, A. S., & Bodurin, M. O. (2014). Corrosion and tribological studies of bamboo leaf ash and alumina reinforced Al-Mg-Si alloy matrix hybrid composites in chloride medium. *International Journal of Electrochemical Science, 9*, 5663–5674.

Ambat, R., Davenport, A. J., Scamans, G. M., & Afseth, A. (2006). Effect of iron-containing intermetallic particles on the corrosion behaviour of aluminium. *Corrosion Science, 48*(11), 3455–3471. https://doi.org/10.1016/j.corsci.2006.01.005

Asif, M., Chandra, K., & Misra, P. S. (2011). Development of aluminium based hybrid metal matrix composites for heavy duty applications. *Journal of Minerals and Materials Characterization and Engineering, 10*(11), 1337–1344.

ASTM G102-89. (2015). *Standard practice for calculation of corrosion rates and related information from electrochemical measurements*. Retrieved May 30, 2017, from http://www.astm.org/Standards/G31

ASTM G1-03. (2011). *Standard practice for preparing, cleaning, and evaluating corrosion test specimens*. Retrieved May 30, 2017, from http://www.astm.org/Standards/G1

ASTM G59-97. (2014). *Standard test method for conducting potentiodynamic polarization resistance measurements*. Retrieved May 30, 2017, from http://www.astm.org/Standards/G31

Aziz, I., Qi, Z., & Min, X. (2009). Corrosion inhibition of SiCp/5A06 aluminum metal matrix composite by cerium conversion treatment. *Chinese Journal of Aeronautics, 22*(6), 670–676. https://doi.org/10.1016/S1000-9361(08)60157-0

Basics of Corrosion Measurements. (xxxx). Retrieved April 6, 2017, from http://www.che.sc.edu/faculty/popov/drbnp/ECHE789b/Corrosion%20Measurements.pdf

Birol, Y. (2007). Response to thermal exposure of the mechanically alloyed Al–Ti/C powders. *Journal of Materials Science, 42*(13), 5123–5128. https://doi.org/10.1007/s10853-006-1263-5

Bodunrin, M. O., Alaneme, K. K., & Chown, L. H. (2015). Aluminium matrix hybrid composites: A review of reinforcement philosophies; mechanical, corrosion and tribological characteristics. *Journal of Materials Research and Technology, 4*(4), 434–445. https://doi.org/10.1016/j.jmrt.2015.05.003

Christian, V. (2004). *Corrosion of aluminium*. New York, NY: Elsevier.

Deuis, R., Green, L., Subramanian, C., & Yellup, J. (1997). Corrosion behavior of aluminum composite coatings. *Corrosion, 53*(11), 880–890. https://doi.org/10.5006/1.3290273

Dobrzański, L. A., Włodarczyk, A., & Adamiak, M. (2005). Structure properties and corrosion resistance of PM composite material based on ENAW-2124 aluminum alloys reinforced with Al_2O_3 ceramic particles. *Journal of Materials Processing Technology, 162–163*, 27–32. https://doi.org/10.1016/j.jmatprotec.2005.02.006

Ehsani, R., & Reihani, S. M. S. (2004). Aging behavior and tensile properties of squeeze cast Al 6061/SiC metal matrix composites. *Scientia Iranica, 11*(4), 392–397.

Gharavi, F., Matori, K. A., Yunus, R., Othman, N. K., & Fadaeifard, F. (2015). Corrosion behavior of Al6061 alloy weldment produced by friction stir welding process. *Journal of Materials Research and Technology, 4*(3), 314–322. https://doi.org/10.1016/j.jmrt.2015.01.007

Gopinath, K., Balasubramaniam, R., & Murthy, V. S. R. (2001). Corrosion behavior of cast Al-Al_2O_3 particulate composites. *Journal of Materials Science Letters, 20*(9), 793–794. https://doi.org/10.1023/A:1010985907514

Guillaumin, V., & Mankowski, G. (2000). Localized corrosion of 6056 T6 aluminium alloy in chloride media. *Corrosion Science, 42*(1), 105–125. https://doi.org/10.1016/S0010-938X(99)00053-0

Paciej, R. C., & Agarwala, V. S. (1986). Metallurgical variables influencing the corrosion susceptibility of a powder metallurgy aluminum/SiCw composite. *Corrosion, 42*(12), 718–729. https://doi.org/10.5006/1.3583046

Prasad, D. S., Shoba, C., & Ramanaiah, N. (2014). Investigations on mechanical properties of aluminum hybrid composites. *Journal of Materials Research and Technology, 3*(1), 79–85. https://doi.org/10.1016/j.jmrt.2013.11.002

Reena Kumari, P. D., Nayak, J., & Nityananda Shetty, A. N. (2016). Corrosion behavior of 6061/Al-15 vol. pct. SiC(p) composite and the base alloy in sodium hydroxide solution. *Arabian Journal of Chemistry, 9*(2), S1144–S1154. https://doi.org/10.1016/j.arabjc.2011.12.003

Singh, J., & Chauhan, A. (2016). Characterization of hybrid aluminum matrix composites for advanced applications – A review. *Journal of Materials Research and Technology, 5*(2), 159–169. https://doi.org/10.1016/j.jmrt.2015.05.004

Trowsdale, A. J., Noble, B., Harris, S. J., Gibbins, I. S. R., Thompson, G. E., & Wood, G. C. (1996). The influence of silicon carbide reinforcement on the pitting behaviour of aluminium. *Corrosion Science, 38*(2), 177–191. https://doi.org/10.1016/0010-938X(96)00098-4

Trzaskoma, P. P. (1990). Pit morphology of aluminum alloy and silicon carbide/aluminum alloy metal matrix composites. *Corrosion, 46*(5), 402–409. https://doi.org/10.5006/1.3585124

Zou, X. G., Miyahara, H., Yamamoto, K., & Ogi, K. (2003). Quantitative evaluation on wear resistance of aluminum alloy composites densely packed with SiC particles. *Materials Science and Technology, 19*(11), 1527–1530. https://doi.org/10.1179/026708303225006015